THE STRUCTURAL DESIGN OF TALL AND SPECIAL BUILDINGS
Struct. Design Tall Spec. Build. **20**, 435–452 (2011)
Published online 6 December 2010 in Wiley Online Library (wileyonlinelibrary.com/journal/tal). DOI: 10.1002/tal.659

Mitigation of wind-induced response of Shanghai Center Tower by tuned mass damper

Xilin Lu and Junru Chen*,†

State Key Laboratory of Disaster Reduction in Civil Engineering, Tongji University, Shanghai, China

SUMMARY

With a height of 632 m, the Shanghai Center Tower, located in Lujiazui district of Shanghai, will be the highest building in China. A tuned mass damper (TMD) system will be set in the upper part of the tower to control the structural wind-induced response. A brief description of fluctuating wind speed simulation is given first. Secondly, analysis of along-wind response of the Shanghai Center Tower was carried out in frequency domain and time domain, through which the wind-induced vibrating comfort of the Shanghai Center Tower and the TMD control performance can be evaluated. Then, the approach that a TMD is installed in the upper part of structure to control the structural wind-induced response and to increase resident comfort of super high-rise building proves to be effective through the analysis results. Copyright © 2010 John Wiley & Sons, Ltd.

1. INTRODUCTION

With a height of 632 m, the Shanghai Center Tower (SHC for short), located in Lujiazui financial district of Shanghai, will be the highest building in China. Designed for commercial, office, hotel and catering, etc., SHC is a composite high-rise building. Figure 1 shows the SHC model constructed for the shaking table test which will be carried out in our laboratory.

Shanghai is located in a coastal area and has been severely hit by typhoon each year. Because of the extreme height, long natural period and low damping, the acceleration response of the upper part of the SHC, where it will be a higher standard hotel, will exceed human comfort limit during wind events. Therefore, a tuned mass damper (TMD) system, the feasibility of which has been verified in practical engineering (Fujino *et al.*, 1996; Soong and Dargush, 1997; Ghorbani-Tanha *et al.*, 2009), will be installed at a height of 565–569 m to suppress the wind-induced motion and to improve the residential comfort of SHC.

Short wind return periods, such as 1–10 years, are usually considered in evaluation of residential comfort of buildings, and a one-year return period is more representative in the regions influenced by typhoons. Therefore, analysis of wind-induced response of SHC was conducted considering wind events of one- and 10-year return periods, respectively.

2. CALCULATION MODEL

Computational model of SHC is essential for numerical analysis in frequency and time domains. Three-dimensional finite element model of SHC created in ETABS, which is a structural analysis software produced by Computers & Structures, Inc., was used for wind-induced vibration analysis, and the model was provided by Thornton Tomasetti, Inc.

*Correspondence to: Junru Chen, State Key Laboratory of Disaster Reduction in Civil Engineering, Tongji University, Shanghai 200092, China
†E-mail: junru03@gmail.com

Figure 1. Shaking table test model of Shanghai center tower.

Table 1. First 10 vibration modes of the tower.

Mode order	Vibration period (s)	Frequency (Hz)	Mode order	Vibration period (s)	Frequency (Hz)
1	8.817	0.113	6	2.013	0.497
2	8.769	0.114	7	1.494	0.670
3	4.152	0.241	8	1.468	0.681
4	3.098	0.323	9	1.248	0.801
5	3.058	0.327	10	0.946	1.057

2.1. Structural dynamic characteristics

Structural dynamic characteristics of SHC are obtained through mode analysis of the ETABS model, which are shown in Table 1. The first two modes are the first-order bending mode in X and Y direction, respectively, and the implementation of a TMD system aims to control the first two modes.

DOI: 10.1002/tal

Table 2. Node division of SHC calculation model.

Node number	Node story	Highest story of node region	Lowest story of node region	Elevation of node story	Height of node region
1	12	10	14	56.8	22.5
2	17	15	19	79.3	22.5
3	22	20	24	103.5	25.2
4	27	25	29	127.0	22.5
5	32	30	34	149.5	22.5
6	37	35	39	173.7	25.2
7	42	40	44	197.2	22.5
8	47	45	49	219.7	22.5
9	52	50	54	243.9	25.2
10	57	55	59	267.4	22.5
11	62	60	64	289.9	22.5
12	67	65	69	314.1	25.2
13	72	70	74	337.6	22.5
14	77	75	79	360.1	22.5
15	82	80	84	383.4	24.2
16	87	85	89	407.4	22.7
17	92	90	94	428.9	21.5
18	97	95	99	450.4	22.5
19	102	100	104	475.4	24.0
20	107	105	109	496.9	21.5
21	112	110	114	518.4	21.5
22	117	115	119	542.0	25.0
23	122	120	124	565.3	21.9
24	Z9–C8	Z9–C5	Z9–C11	591.1	30.1
25	Z9–C15	Z9–C12	Z9–C18	621.2	30.1

2.2. Simplification of wind loads action on the structure

Because the story number of SHC is quite large, it is unnecessary to apply wind loads on every story, which will significantly increase the computational complexity. In this paper, the wind loads acting model are simplified as 25 nodes model, and the wind loads acting on several stories are applied at the node story. The node division data are given in Table 2.

3. SIMULATION OF FLUCTUATING WIND LOAD

Time series of fluctuating wind load on SHC, which can be derived from time series of fluctuating wind speed at the site of SHC, are essential for the time history analysis of wind-induced responses. Considering that measured time series data of wind speed above 300 m are too less to be used for time history analysis directly and the wind tunnel test of SHC did not give the time series of fluctuating wind load but the maximum one, it is necessary to simulate the fluctuating wind load on SHC.

3.1. Simulation assumption

Observation records of wind speed indicate that wind speed is composed of two parts: mean wind whose predominant period is above 10 minutes and fluctuating wind whose predominant period is about several seconds. With precondition of meeting requirements of calculation precision, the following assumptions (Simiu and Scanlan, 1996) can be made:

(a) mean wind speed at any point of the building does not change with time.
(b) fluctuating wind speed is a stable random process with zero mean.
(c) wind speed at different points of the building has spatial correlation with each other.

DOI: 10.1002/tal

Fluctuation wind can induce along-wind vibration and crosswind vibration of structure, and vortex-induced vibration is the main kind of crosswind vibration. With the consideration that the crosswind loads cannot be simulated accurately through numerical technology and this paper focuses on the TMD performance not the wind-resistant design, the along-wind component of wind-induced response of SHC was only taken account in this paper, which has little influence on the analytical results.

3.2. Basic parameters of wind load

Wind mean speed profile used in wind tunnel test was adopted, which is given in Table 3. Karman wind speed spectrum was used as the along-wind speed spectrum for simulation, which is given as (Simiu and Scanlan, 1996)

$$S_u(z,n) = 4\sigma_u^2 \frac{f}{n(1+70.8f^2)^{5/6}} \tag{1}$$

where $S_u(z,n)$ is the PSD of fluctuating wind speed; n is the frequency of wind; z denotes the height; $\sigma_u^2 = 6k\bar{\psi}_{10}^2$; $f = \dfrac{nL_u(z)}{\bar{v}_z}$, in which $L_u(z) = 100\left(\dfrac{z}{30}\right)^{0.5}$; k is the roughness coefficient of ground.

The surface of SHC is formed via rotation with height of plane shape, which is a triangle with arcs. Four cases of wind directions are the most unfavourable, which are shown in Figure 2. The exact

Table 3. Mean speed profile used in wind tunnel test.

Height (m)	V_z/V_{500}	Height (m)	V_z/V_{500}
25.4	0.42	177.8	0.82
38.1	0.50	203.2	0.85
50.8	0.58	254.0	0.89
63.5	0.62	304.8	0.92
76.2	0.66	355.6	0.96
88.9	0.68	406.4	0.98
101.6	0.71	457.2	0.99
127.0	0.77	508.0	1.01
152.4	0.79	609.6	1.06

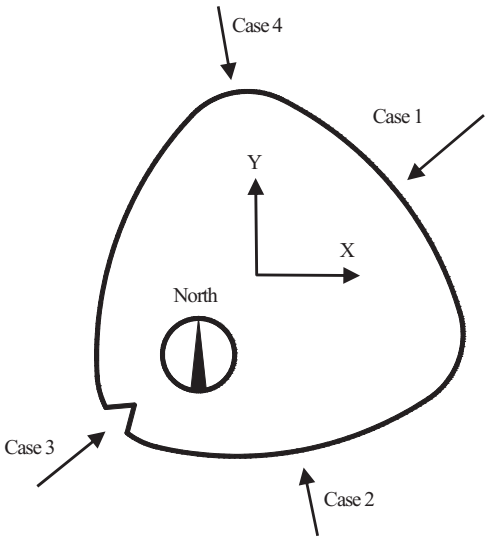

Figure 2. Four cases of wind direction for calculation.

DOI: 10.1002/tal

Table 4. Parameters of fluctuating wind speed simulation.

Parameters	One-year return period	10-year return period
Gradient wind speed (m/s)	25.8	36.3
Order of AR model	5	5
Sampling frequency (Hz)	1.25	1.25
Time step (s)	0.8	0.8
Duration of wind speed (s)	1200	1200

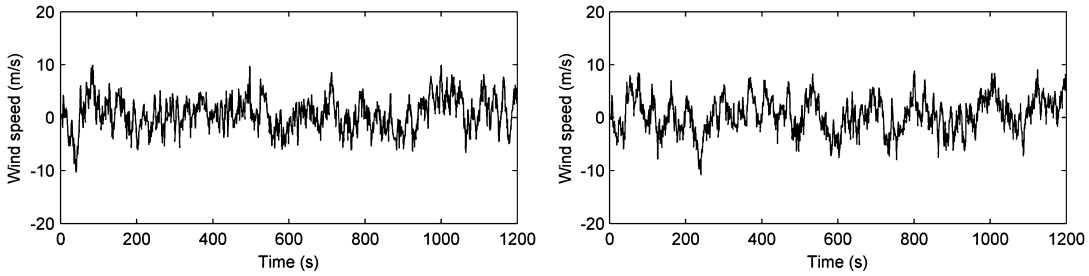

Figure 3. Time–history curves of fluctuating wind speed of one-year return period.

direction of each case is based on the bottom cross-section, and wind tunnel data of shape coefficients of SHC in different cases were used for calculation in the paper.

3.3. Simulation of fluctuating wind speed

Linear filtering method and harmony superposition method are the most widely used for simulating fluctuating wind speed (Iannuzzi and Spinelli, 1987). Based on the summation of trigonometric series, harmony superposition method uses discrete spectrum to approach the target spectrum, which will take much computation time and cannot take spatial correlation into account. Different from harmony superposition method, linear filtering method is based on digital filtering technique, which inputs a white noise random sequence to a designed linear filter and outputs a random sequence with features of assigned spectrums.

Auto-regressive model is widely used in linear filtering method and has proved to be very effective and accurate in simulation of wind speed with features of randomness, temporal and special correlation by previous studies. We obtained the time series of fluctuating wind speed on SHC through digital simulation in MATLAB, which is a software of high-level language and interactive programming environment produced by The MathWorks company, and then got the fluctuating wind load acting on SHC through transformation from the fluctuating wind speed. The parameters of wind speed simulation are given in Table 4, and Figure 3 shows the wind speed time history curves of a one-year return period.

4. ANALYSIS OF WIND-INDUCED RESPONSE

4.1. Analytical parameters

The results of the model analysis show that the first-order vibration frequencies in the X and Y directions are 0.113 Hz and 0.114 Hz, respectively.

As the wind-induced motion of SHC is dominated by first-order mode in the X and Y directions, the damping ratios of different modes can be the same value. In Smith and Willford (2007, 2008),

DOI: 10.1002/tal

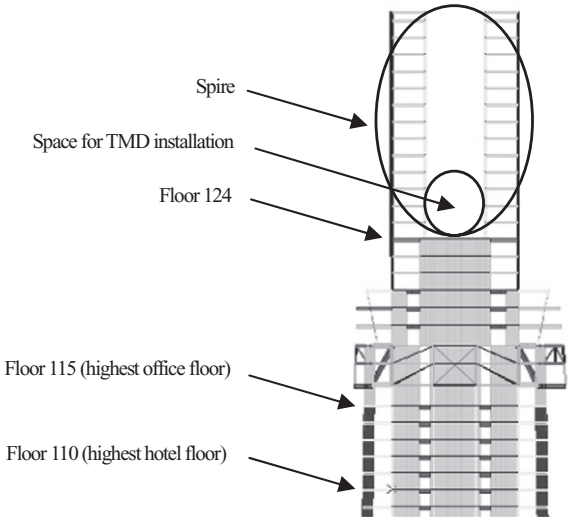

Figure 4. Positions of the TMD system.

Table 5. Optimal parameters of TMD system in four wind direction cases.

		X direction		*Y* direction	
TMD mass	Wind direction cases	Optimal damping ratio	Optimal frequency ratio	Optimal damping ratio	Optimal frequency ratio
1400 t	Case 1	0.0507	0.9993	0.0505	0.9996
	Case 2	0.0500	1.0000	0.0585	0.9906
	Case 3	0.0507	0.9993	0.0504	0.9996
	Case 4	0.0500	1.0000	0.0584	0.9906

based on the actual measure data, the damping ratio of supper high-rise buildings is usually smaller than 0.01, which is commonly used in design stage. However, as SHC is being designed, the exact value of structural damping ratio can not be determined, and 0.01 is adopted as the structural damping ratio in the paper according to the wind tunnel test's suggestion.

A TMD system will be installed on the 124th floor, the mass of which is 1400 tons according to the conceptual design of TMD system proposed by Rowan Williams Davies & Irwin Inc. (RWDI), and Figure 4 illustrates the position of the TMD system. Through parameter optimization in four wind direction cases, the optimal TMD parameters were obtained, which are given in Table 5.

4.2. Comfort criteria

The comfort criteria for the SHC are defined as the limitations of structure vibration acceleration during wind events of 10-year return period, which are given by Chinese codes as

On office stories:

$$\alpha_{\max} = 0.25 m/s^2$$

On hotel stories:

$$\alpha_{\max} = 0.15 m/s^2$$

With the consideration of the importance of structure itself and higher standard hotel services provided by the SHC, the comfort criteria are improved to

DOI: 10.1002/tal

On office stories:

$$\alpha_{\max} = 0.15 m/s^2$$

On hotel stories:

$$\alpha_{\max} = 0.10 m/s^2$$

The highest office story and hotel story are on the 115th story (531.3 m) and 110th story (509.8 m), respectively. For the higher the story is the larger response will occur in wind events, evaluation of residential comfort on these two stories is enough for the whole building of SHC.

4.3. Formulation

Because of the symmetry and high slenderness ratio, the SHC can be modelled as a vertical linear cantilever beam with N DOFs (DOF is the abbreviation of 'degree of freedom'). It is assumed that a TMD whose mass, damping and stiffness are denoted by m_d, c_d and k_d, respectively, is connected to the ith DOF of the SHC. The tower with the attached TMD can be treated as an $N + 1$ DOF system and its motion equations can be written as

$$\boldsymbol{M}\ddot{\boldsymbol{x}} + \boldsymbol{C}\dot{\boldsymbol{x}} + \boldsymbol{K}\boldsymbol{x} = \boldsymbol{P}(t) + \boldsymbol{E}(c_d\dot{v} + k_d v) \tag{2}$$

$$m_d\ddot{v} + c_d\dot{v} + k_d v = -m_d E\{\ddot{x}\} \tag{3}$$

where $\boldsymbol{M}$, $\boldsymbol{C}$ and $\boldsymbol{K}$ are the mass, damping and stiffness matrixes of the structure, respectively; $\boldsymbol{x}$ is an N-dimensional displacement vector of the structure; x_d is the displacement of the TMD; $\boldsymbol{P}(t)$ is an N-dimensional wind excitation vector; E is an N-dimensional location vector of control force, whose ith component is 1 and the other components are 0; v is the relative displacement of the TMD with respect to the ith DOF of structure, given by $v = x_d - x_i$.

Previous studies point out that the vibration of high-rise building is dominated by first mode under wind excitation so the wind-induced displacement of structure can be given as

$$\mathbf{x} \approx \boldsymbol{\varphi}_1 q_1(t) \tag{4}$$

where $\boldsymbol{\varphi}_1$ is the first-order mode vector of structure; $q_1(t)$ is the first-order generalized coordinate of structure.

Based on the orthogonality of vibration modes with respect to mass, damping and stiffness matrixes, the motion equations of system can be derived as

$$\ddot{q}_1 + 2\zeta_1\omega_1\dot{q}_1 + \omega_1^2 q_1 = F_1(t) + \mu_1\varphi_{1i}(2\zeta_d\omega_d\dot{v} + \omega_d^2 v) \tag{5}$$

$$\ddot{v} + 2\zeta_d\omega_d\dot{v} + \omega_d^2 v = -\varphi_{1i}\ddot{q}_1 \tag{6}$$

where ω_1 and ζ_1 is the circle frequency and the damping ratio of mode 1, respectively; ω_d and ζ_d is the circle frequency and the damping ratio of the TMD system, respectively; μ_1 is the generalized mass ratio of the TMD mass with respect to the generalized mass of mode 1; φ_{1i} is the ith element of mode 1 vector; $F_1(t)$ is the generalized wind excitation, given by

$$F_1(t) = \boldsymbol{\varphi}_1^T \boldsymbol{P}(t)/M_1 \tag{7}$$

in which M_1 denotes the generalized mass of mode1.

Equations (5) and (6) can be expressed in the form of a matrix as

$$\begin{bmatrix} 1+\mu_1\varphi_{1i}^2 & \mu_1\varphi_{1i} \\ \varphi_{1i} & 1 \end{bmatrix}\begin{Bmatrix} \ddot{q}_1 \\ \ddot{v} \end{Bmatrix} + \begin{bmatrix} 2\zeta_1\omega_1 & 0 \\ 0 & 2\zeta_d\omega_d \end{bmatrix}\begin{Bmatrix} \dot{q}_1 \\ \dot{v} \end{Bmatrix} + \begin{bmatrix} \omega_1^2 & 0 \\ 0 & \omega_d^2 \end{bmatrix}\begin{Bmatrix} q_1 \\ v \end{Bmatrix} = \begin{Bmatrix} F_1(t) \\ 0 \end{Bmatrix} \tag{8}$$

Substituting $e^{i\omega t}$ for $F_1(t)$, the frequency response function of structural generalized coordinate and the TMD relative displacement can be derived as the following equations, respectively

DOI: 10.1002/tal

$$H_{q1}(i\omega) = \frac{1}{D}[(\omega_d^2 - \omega^2) + 2\zeta_d\omega_d(i\omega)] \tag{9}$$

$$H_v(i\omega) = \frac{1}{D}\varphi_{1i}\omega^2 \tag{10}$$

in which

$$D = \omega^4 - 2(\zeta_1\omega_1 + \zeta_d\omega_d + \mu_1\varphi_{1i}^2\zeta_d\omega_d)\cdot(\omega_1^2 + \omega_d^2 + \mu_1\varphi_{1i}^2\omega_d^2 + 4\xi_1\omega_1\zeta_d\omega_d)\cdot\omega^2$$
$$+2(\zeta_1\omega_1\omega_d^2 + \zeta_d\omega_d\omega_1^2)\cdot i\omega + \omega_1^2\omega_d^2.$$

Then, the transfer functions of structural generalized coordinate and the TMD relative displacement can be obtained, respectively, given by

$$|H_{q1}(i\omega)|^2 = \frac{1}{E}\left[\left(\lambda_1^2 - \left(\frac{\omega}{\omega_1}\right)^2\right)^2 + 4\zeta_d^2\lambda_1^2\left(\frac{\omega}{\omega_1}\right)^2\right] \tag{11}$$

$$|H_v(i\omega)|^2 = \frac{1}{E}\varphi_{1i}^2\left(\frac{\omega}{\omega_1}\right)^4 \tag{12}$$

in which

$$E = \omega_1^4\left\{\left[\left(\frac{\omega}{\omega_1}\right)^4 - ((1+\mu_1\phi_{1i}^2)\lambda_1^2 + 4\zeta_1\zeta_d\lambda_1 + 1)\left(\frac{\omega}{\omega_1}\right)^2 + \lambda_1^2\right]^2\right.$$
$$\left.+4\left[((1+\mu_1\varphi_{1i}^2)\zeta_d\lambda_1 + \zeta_1)\left(\frac{\omega}{\omega_1}\right)^2 - (\zeta_1\lambda_1^2 + \zeta_d\lambda_1)\left(\frac{\omega}{\omega_1}\right)\right]^2\right\}$$

where λ_1 is the frequency ratio, given by $\lambda = \omega_d/\omega_1$.

The transfer function of uncontrolled structure is defined as

$$|H_{q1}^0(i\omega)|^2 = \frac{1}{(\omega^2 - \omega_1^2)^2 + (2\zeta_1\omega_1\omega)^2} \tag{13}$$

According to random vibration theory, the variance of wind-induced displacement and acceleration of kth story is defined, respectively, as

$$(\sigma_{x_k}^0)^2 = \varphi_{1k}^2\int_{-\infty}^{+\infty}|H_{q1}^0(i\omega)|^2 S_f(\omega)d\omega \tag{14}$$

$$(\sigma_{\ddot{x}_k}^0)^2 = \varphi_{1k}^2\int_{-\infty}^{+\infty}\omega^4|H_{q1}^0(i\omega)|^2 S_f(\omega)d\omega \tag{15}$$

where $S_f(\omega)$ is the generalized power spectrum density of wind load in respect of mode 1.

For the structure controlled by the TMD system, the response variance of structure and the TMD can be given as the following equations

$$(\sigma_{x_k})^2 = \varphi_{1k}^2\int_{-\infty}^{+\infty}|H_{q1}(i\omega)|^2 S_f(\omega)d\omega \tag{16}$$

$$(\sigma_{\ddot{x}_k})^2 = \varphi_{1k}^2\int_{-\infty}^{+\infty}\omega^4|H_{q1}(i\omega)|^2 S_f(\omega)d\omega \tag{17}$$

$$v^2 = \int_{-\infty}^{+\infty}|H_v(i\omega)|^2 S_f(\omega)d\omega \tag{18}$$

In order to evaluate the effectiveness of the TMD on the response reduction of the SHC, two non-dimensional evaluation criteria are considered called displacement reduction ratio and accelera-

DOI: 10.1002/tal

Table 6. Wind-induced responses of one-year return period in case 1 (gradient wind speed: 25.8 m/s)

		X direction		Y direction	
Story	Response	Uncontrolled	TMD controlled	Uncontrolled	TMD controlled
115	Variance of displacement (cm^2)	9.24	5.45	5.86	3.50
	Displacement reduction ratio		0.59		0.60
	Maximum displacement (cm)	7.84	6.02	6.25	4.83
	Variance of acceleration (cm^2/s^4)	1.26	0.34	0.54	0.24
	Acceleration reduction ratio		0.27		0.44
	Maximum acceleration (cm/s^2)	2.90	1.51	1.89	1.26
110	Variance of displacement (cm^2)	7.97	4.70	5.06	3.02
	Displacement reduction ratio		0.59		0.60
	Maximum displacement (cm)	7.28	5.59	5.80	4.48
	Variance of acceleration (cm^2/s^4)	1.09	0.30	0.46	0.20
	Acceleration reduction ratio		0.27		0.44
	Maximum acceleration (cm/s^2)	2.69	1.40	1.75	1.17
124 (Location of TMD)	Variance of relative displacement of TMD (cm^2)		69.55		43.71
	Maximum relative displacement of TMD (cm)		21.52		17.06

tion reduction ratio, respectively. The two evaluation criteria are defined by the TMD's ability to reduce the response variance of structural displacement and acceleration and are given, respectively, by

$$\delta_{x_k}^2 = \frac{(\sigma_{x_k})^2}{(\sigma_{x_k}^0)^2} \tag{19}$$

$$\delta_{\ddot{x}_k}^2 = \frac{(\sigma_{\ddot{x}_k})^2}{(\sigma_{\ddot{x}_k}^0)^2} \tag{20}$$

4.4. Frequency domain analysis

Substituting relevant parameters in Equations (14)–(18), the response variances of wind-induced displacement and acceleration of the SHC and the TMD can be calculated. Based on random vibration theory (Clough and Penzien, 1993), the structural response under wind excitation is random variables of normal distribution with zero means, and the maximum response is defined as the value of 99.5% probability given as

$$x_{\max} = 2.58\sigma_x \tag{21}$$

Through numerical calculations in MATLAB, the responses of structure and the TMD in four wind cases were obtained, which are given in Tables 6–13. The time spent in each wind case was about 450 s, which has confirmed the efficiency of frequency domain analysis. From the results in frequency domain analysis, we can find that the wind-induced responses are larger in cases 1 and 3 in the X direction, and cases 2 and 4 in the Y direction so the final control parameters of the TMD system are determined by the optimal results of cases 1 and 4 in the X and Y directions, respectively, which is given in Table 14.

4.5. Time history analysis

Compared with frequency analysis, time history analysis, though having lower computational efficiency, can obtain more accurate and visual wind-induced response of structure and the TMD. Besides,

DOI: 10.1002/tal

Table 7. Wind-induced responses of one-year return period in case 2 (gradient wind speed: 25.8 m/s).

		X direction		*Y* direction	
Story	Response	Uncontrolled	TMD controlled	Uncontrolled	TMD controlled
115	Variance of displacement (cm^2)	0.52	0.29	17.66	10.31
	Displacement reduction ratio		0.57		0.58
	Maximum displacement (cm)	1.86	1.40	10.84	8.28
	Variance of acceleration (cm^2/s^4)	0.03	0.02	2.58	0.70
	Acceleration reduction ratio		0.56		0.27
	Maximum acceleration (cm/s^2)	0.43	0.33	4.14	2.15
110	Variance of displacement (cm^2)	0.45	0.25	15.23	8.89
	Displacement reduction ratio		0.57		0.58
	Maximum displacement (cm)	1.73	1.30	10.07	7.69
	Variance of acceleration (cm^2/s^4)	0.02	0.01	2.22	0.60
	Acceleration reduction ratio		0.56		0.27
	Maximum acceleration (cm/s^2)	0.40	0.30	3.85	2.00
124 (Location of TMD)	Variance of relative displacement of TMD (cm^2)		4.09		118.24
	Maximum relative displacement of TMD (cm)		5.22		28.05

Table 8. Wind-induced responses of one-year return period in case 3 (gradient wind speed: 25.8 m/s).

		X direction		*Y* direction	
Story	Response	Uncontrolled	TMD controlled	Uncontrolled	TMD controlled
115	Variance of displacement (cm^2)	9.25	5.47	5.55	3.32
	Displacement reduction ratio		0.59		0.60
	Maximum displacement (cm)	7.85	6.03	6.08	4.70
	Variance of acceleration (cm^2/s^4)	1.26	0.34	0.51	0.22
	Acceleration reduction ratio		0.27		0.44
	Maximum acceleration (cm/s^2)	2.89	1.51	1.83	1.22
110	Variance of displacement (cm^2)	7.98	4.72	4.79	2.86
	Displacement reduction ratio		0.59		0.60
	Maximum displacement (cm)	7.29	5.60	5.65	4.37
	Variance of acceleration (cm^2/s^4)	1.09	0.30	0.44	0.19
	Acceleration reduction ratio		0.27		0.44
	Maximum acceleration (cm/s^2)	2.69	1.40	1.70	1.13
124 (Location of TMD)	Variance of relative displacement of TMD (cm^2)		69.44		41.29
	Maximum relative displacement of TMD (cm)		21.50		16.58

as the computational technology has been developing rapidly, the time spent on time history analysis has become shorter and shorter.

The TMD system was simulated in the three-dimensional finite element model of the SHC created in the ETABS program, which is essential for time history analysis. Because time history analysis in the ETABS program is based on the mode analysis in which the model DOFs correspond to each story; an extra story was set on which the TMD mass locates. Then, the TMD mass was simulated by a mass point. A dual pendulum TMD system, which is an improved form of traditional pendulum systems, is adopted as the form of TMD in SHC. However, since the simulation of the TMD mass

DOI: 10.1002/tal

Table 9. Wind-induced responses of one-year return period in case 4 (gradient wind speed: 25.8 m/s).

		X direction		*Y* direction	
Story	Response	Uncontrolled	TMD controlled	Uncontrolled	TMD controlled
115	Variance of displacement (cm^2)	0.58	0.34	18.29	10.68
	Displacement reduction ratio		0.58		0.58
	Maximum displacement (cm)	1.97	1.50	11.04	8.43
	Variance of acceleration (cm^2/s^4)	0.03	0.02	2.67	0.72
	Acceleration reduction ratio		0.56		0.27
	Maximum acceleration (cm/s^2)	0.46	0.34	4.22	2.19
110	Variance of displacement (cm^2)	0.50	0.29	15.77	9.21
	Displacement reduction ratio		0.58		0.58
	Maximum displacement (cm)	1.83	1.39	10.25	7.83
	Variance of acceleration (cm^2/s^4)	0.03	0.02	2.30	0.62
	Acceleration reduction ratio		0.56		0.27
	Maximum acceleration (cm/s^2)	0.42	0.32	3.92	2.04
124 (Location of TMD)	Variance of relative displacement of TMD (cm^2)		4.51		122.56
	Maximum relative displacement of TMD (cm)		5.48		28.56

Table 10. Wind-induced responses of 10-year return period in case 1 (gradient wind speed: 36.3 m/s).

		X direction		*Y* direction	
Story	Response	Uncontrolled	TMD controlled	Uncontrolled	TMD controlled
115	Variance of displacement (cm^2)	49.27	25.09	31.17	16.06
	Displacement reduction ratio		0.51		0.52
	Maximum displacement (cm)	18.11	12.92	14.40	10.34
	Var iance of acceleration (cm^2/s^4)	8.03	2.18	5.34	1.45
	Acceleration reduction ratio		0.27		0.27
	Maximum acceleration (cm/s^2)	7.31	3.81	5.96	3.11
110	Variance of displacement (cm^2)	42.48	21.63	26.87	13.85
	Displacement reduction ratio		0.51		0.52
	Maximum displacement (cm)	16.82	12.00	13.37	9.60
	Variance of acceleration (cm^2/s^4)	6.93	1.88	4.61	1.25
	Acceleration reduction ratio		0.27		0.27
	Maximum acceleration (cm/s^2)	6.79	3.54	5.54	2.89
124 (Location of TMD)	Variance of relative displacement of TMD (cm^2)		443.93		279.31
	Maximum relative displacement of TMD (cm)		54.36		43.12

point suspended by lines is treated as an unstable system, the pendulum system of the TMD could not be simulated exactly in ETABS program, and we used spring line elements linked to the mass point to provide stiffness of the TMD system. Meanwhile, each viscous damper of the TMD system was simulated by a line with link property of damper.

After the modelling of the TMD system, time history analysis in different wind cases was carried out in the ETABS program, and the results are close to that of frequency domain analysis. Tables 15–22 shows the maximum response of structure and the TMD, and Figures 5–8 display the time history curves of wind-induced response of structure.

DOI: 10.1002/tal

Table 11. Wind-induced response of 10-year return period in case 2 (gradient wind speed: 36.3 m/s).

		X direction		*Y* direction	
Story	Response	Uncontrolled	TMD controlled	Uncontrolled	TMD controlled
115	Variance of displacement (cm^2)	2.78	1.38	94.19	47.43
	Displacement reduction ratio		0.50		0.50
	Maximum displacement (cm)	4.30	3.03	25.04	17.77
	Variance of acceleration (cm^2/s^4)	0.47	0.13	16.39	4.41
	Acceleration reduction ratio		0.28		0.27
	Maximum acceleration (cm/s^2)	1.76	0.93	10.44	5.42
110	Variance of displacement (cm^2)	2.39	1.19	81.22	40.89
	Displacement reduction ratio		0.50		0.50
	Maximum displacement (cm)	3.99	2.82	23.25	16.50
	Variance of acceleration (cm^2/s^4)	0.40	0.11	14.13	3.80
	Acceleration reduction ratio		0.28		0.27
	Maximum acceleration (cm/s^2)	1.64	0.86	9.70	5.03
124 (Location of TMD)	Variance of relative displacement of TMD (cm^2)		25.85		752.59
	Maximum relative displacement of TMD (cm)		13.12		70.78

Table 12. Wind-induced response of 10-year return period in case 3 (gradient wind speed: 36.3 m/s).

		X direction		*Y* direction	
Story	Response	Uncontrolled	TMD controlled	Uncontrolled	TMD controlled
115	Variance of displacement (cm^2)	49.33	25.17	29.51	15.24
	Displacement reduction ratio		0.51		0.52
	Maximum displacement (cm)	18.12	12.94	14.02	10.07
	Variance of acceleration (cm^2/s^4)	8.03	2.18	5.05	1.37
	Acceleration reduction ratio		0.27		0.27
	Maximum acceleration (cm/s^2)	7.31	3.81	5.80	3.02
110	Variance of displacement (cm^2)	42.54	21.70	25.44	13.14
	Displacement reduction ratio		0.51		0.52
	Maximum displacement (cm)	16.83	12.02	13.01	9.35
	Variance of acceleration (cm^2/s^4)	6.92	1.88	4.35	1.18
	Acceleration reduction ratio		0.27		0.27
	Maximum acceleration (cm/s^2)	6.79	3.53	5.38	2.81
124 (Location of TMD)	Variance of relative displacement of TMD (cm^2)		443.61		263.96
	Maximum relative displacement of TMD (cm)		54.34		41.92

From the analysis results in frequency domain and time domain, we can find that

(a) In wind events of one-year return period, the acceleration response of uncontrolled structure is within the residential comfort limit, and the maximum displacement and acceleration of structure controlled by the TMD is reduced to 47–61% and 33–42% of uncontrolled response, respectively.
(b) In wind events of 10-year return period, the acceleration response of uncontrolled structure exceeds the residential comfort limit, but the response of structure was controlled to satisfy residential comfort requirement after the TMD system was attached to SHC, and the maximum

DOI: 10.1002/tal

Table 13. Wind-induced response of 10-year return period in case 4 (gradient wind speed: 36.3 m/s).

Story	Response	*X* direction		*Y* direction	
		Uncontrolled	TMD controlled	Uncontrolled	TMD controlled
115	Variance of displacement (cm^2)	3.11	1.56	97.59	49.12
	Displacement reduction ratio		0.50		0.50
	Maximum displacement (cm)	4.55	3.23	25.49	18.08
	Variance of acceleration (cm^2/s^4)	0.52	0.14	16.98	4.57
	Acceleration reduction ratio		0.28		0.27
	Maximum acceleration (cm/s^2)	1.86	0.98	10.63	5.51
110	Variance of displacement (cm^2)	2.68	1.35	84.15	42.36
	Displacement reduction ratio		0.50		0.50
	Maximum displacement (cm)	4.23	3.00	23.67	16.79
	Variance of acceleration (cm^2/s^4)	0.45	0.12	14.64	3.94
	Acceleration reduction ratio		0.28		0.27
	Maximum acceleration (cm/s^2)	1.72	0.91	9.87	5.12
124 (Location of TMD)	Variance of relative displacement of TMD (cm^2)		28.67		780.15
	Maximum relative displacement of TMD (cm)		13.81		72.06

Table 14. Final control parameters of TMD system.

Parameters	Value	
	X direction	Y direction
Mass (t)	1400	1400
Mass ratio	0.0172	0.0172
Damping ratio	0.0507	0.0585
Damping coefficient (kN s/m)	99.17	115.14
Frequency ratio	0.9993	0.9906
Period (s)	8.991	8.931
Stiffness (kN/m)	683.68	692.93
Pendulum length (m)	20.13	19.86
Equivalent damping ratio	0.0363	0.0368

Table 15. Maximum response of one-year return period in case 1 (gradient wind speed: 25.8 m/s).

Response		X direction			Y direction		
		Uncontrolled	TMD controlled	Reduction ratio (%)	Uncontrolled	TMD controlled	Reduction ratio (%)
Story 115	Displacement (cm)	10.3	6.0	58.3	9.8	4.7	48.0
	Acceleration (cm/s^2)	6.0	2.0	33.3	3.7	1.4	37.8
Story 110	Displacement (cm)	9.6	5.6	58.3	9.2	4.3	46.7
	Acceleration (cm/s^2)	5.5	1.9	34.5	3.6	1.2	33.3
Relative displacement of TMD (cm)			24.5			20.1	

DOI: 10.1002/tal

Table 16. Maximum response of one-year return period in case 2 (gradient wind speed: 25.8 m/s).

	X direction			Y direction		
Response	Uncontrolled	TMD controlled	Reduction ratio (%)	Uncontrolled	TMD controlled	Reduction ratio (%)
Story 115 Displacement (cm)	2.3	1.4	60.9	17.2	8.1	47.1
Acceleration (cm/s^2)	1.4	0.5	35.7	6.3	2.6	41.3
Story 110 Displacement (cm)	2.2	1.3	59.1	16.1	7.5	46.6
Acceleration (cm/s^2)	1.2	0.5	41.7	6.2	2.3	37.1
Relative displacement of TMD (cm)		5.6			34.6	

Table 17. Maximum response of one-year return period in case 3 (gradient wind speed: 25.8 m/s).

	X direction			Y direction		
Response	Uncontrolled	TMD controlled	Reduction ratio (%)	Uncontrolled	TMD controlled	Reduction ratio (%)
Story 115 Displacement (cm)	10.3	5.9	57.3	9.6	4.5	46.9
Acceleration (cm/s^2)	5.9	2.0	33.9	3.6	1.4	38.9
Story 110 Displacement (cm)	9.6	5.5	57.3	8.9	4.2	47.2
Acceleration (cm/s^2)	5.5	1.8	32.7	3.5	1.2	34.3
Relative displacement of TMD (cm)		24.6			19.5	

Table 18. Maximum response of one-year return period in case 4 (gradient wind speed: 25.8 m/s).

	X direction			Y direction		
Response	Uncontrolled	TMD controlled	Reduction ratio (%)	Uncontrolled	TMD controlled	Reduction ratio (%)
Story 115 Displacement (cm)	2.5	1.5	60.0	17.6	8.2	46.6
Acceleration (cm/s^2)	1.5	0.5	33.3	6.5	2.7	41.5
Story 110 Displacement (cm)	2.3	1.4	60.9	16.4	7.7	47.0
Acceleration (cm/s^2)	1.3	0.5	38.5	6.3	2.4	38.1
Relative displacement of TMD (cm)		6.0			35.3	

Table 19. Maximum response of 10-year return period in case 1 (gradient wind speed: 36.3 m/s).

	X direction			*Y* direction		
Response	Uncontrolled	TMD controlled	Reduction ratio (%)	Uncontrolled	TMD controlled	Reduction ratio (%)
Story 115 Displacement (cm)	20.0	13.8	69.0	18.3	12.5	68.3
Acceleration (cm/s^2)	7.8	4.5	57.7	6.5	3.5	53.8
Story 110 Displacement (cm)	18.7	12.8	68.4	17.1	11.6	67.8
Acceleration (cm/s^2)	6.9	3.8	55.1	5.9	3.2	54.2
Relative displacement of TMD (cm)		49.0			46.5	

DOI: 10.1002/tal

Table 20. Maximum response of 10-year return period in case 2 (gradient wind speed: 36.3 m/s).

Response		*X* direction			*Y* direction		
		Uncontrolled	TMD controlled	Reduction ratio (%)	Uncontrolled	TMD controlled	Reduction ratio (%)
Story 115	Displacement (cm)	4.3	3.1	72.1	32.1	21.7	67.6
	Acceleration (cm/s^2)	1.7	0.9	52.9	11.3	6.0	53.1
Story 110	Displacement (cm)	4.0	3.1	77.5	30.0	20.3	67.7
	Acceleration (cm/s^2)	1.5	0.9	60.0	10.2	5.5	53.9
Relative displacement of TMD (cm)			11.7			80.3	

Table 21. Maximum response of 10-year return period in case 3 (gradient wind speed: 36.3 m/s).

Response		*X* direction			*Y* direction		
		Uncontrolled	TMD controlled	Reduction ratio (%)	Uncontrolled	TMD controlled	Reduction ratio (%)
Story 115	Displacement (cm)	20.2	13.8	68.3	17.7	12.1	67.6
	Acceleration (cm/s^2)	7.8	4.7	60.3	6.4	3.5	53.1
Story 110	Displacement (cm)	18.8	12.9	68.6	16.6	11.3	67.7
	Acceleration (cm/s^2)	6.9	3.9	56.5	5.7	3.1	53.9
Relative displacement of TMD (cm)			49.1			45.3	

Table 22. Maximum response of 10-year return period in case 4 (gradient wind speed: 36.3 m/s).

Response		*X* direction			*Y* direction		
		Uncontrolled	TMD controlled	Reduction ratio (%)	Uncontrolled	TMD controlled	Reduction ratio (%)
Story 115	Displacement (cm)	4.7	3.5	74.5	32.6	22.1	67.8
	Acceleration (cm/s^2)	1.9	1.0	52.6	11.4	6.2	54.4
Story 110	Displacement (cm)	4.4	3.2	72.7	30.5	20.6	67.5
	Acceleration (cm/s^2)	1.6	0.9	56.3	10.3	5.6	54.4
Relative displacement of TMD (cm)			12.2			81.9	

displacement and acceleration of structure controlled by the TMD is reduced to 68–78% and 53–61% of uncontrolled response, respectively.

Though the TMD system was equipped mainly to control the acceleration response of structure, the displacement response could be reduced to some extent, which guarantees the safety of structure during wind events.

Aimed to study the influence of structural damping ratios on TMD control performance, time history analysis in case 4 excited by 10-year wind event with different structural damping ratios were carried out in the ETABS program, and the results are shown in Figure 9. From the results, we can find that the wind-induced response decreases rapidly as the structural damping ratio increases, but the response changes with the structural damping ratio to a lesser extent after the TMD system has been installed, which leads to the decease of TMD control performance with the structural damping ratio. Therefore, the TMD is more suitable to control the buildings of low damping ratios.

DOI: 10.1002/tal

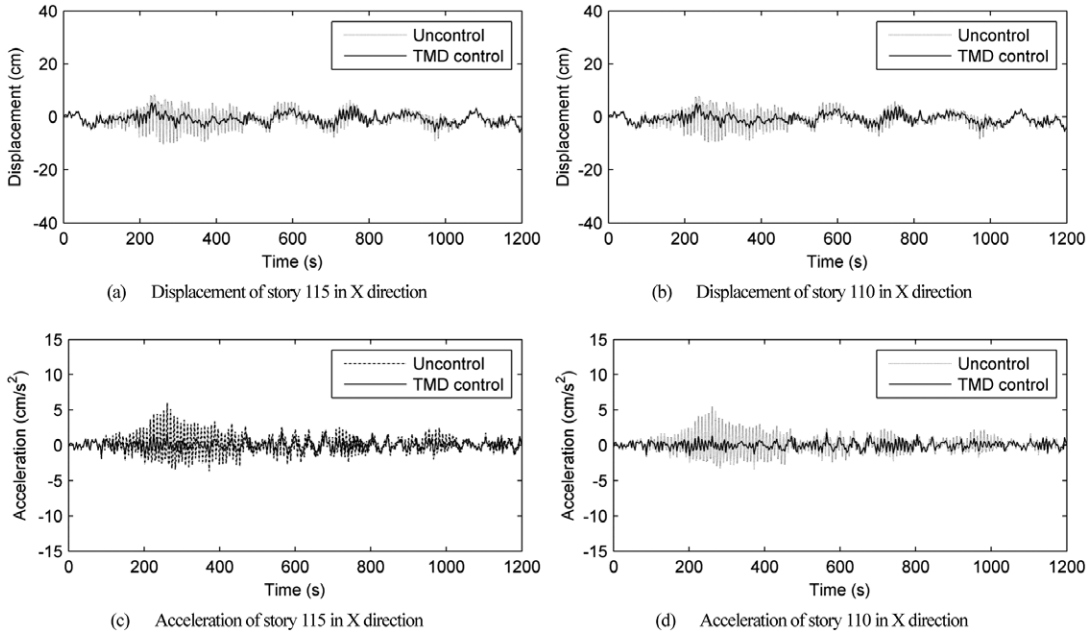

Figure 5. Time–history curves of structural response induced by one-year wind event in case 1.

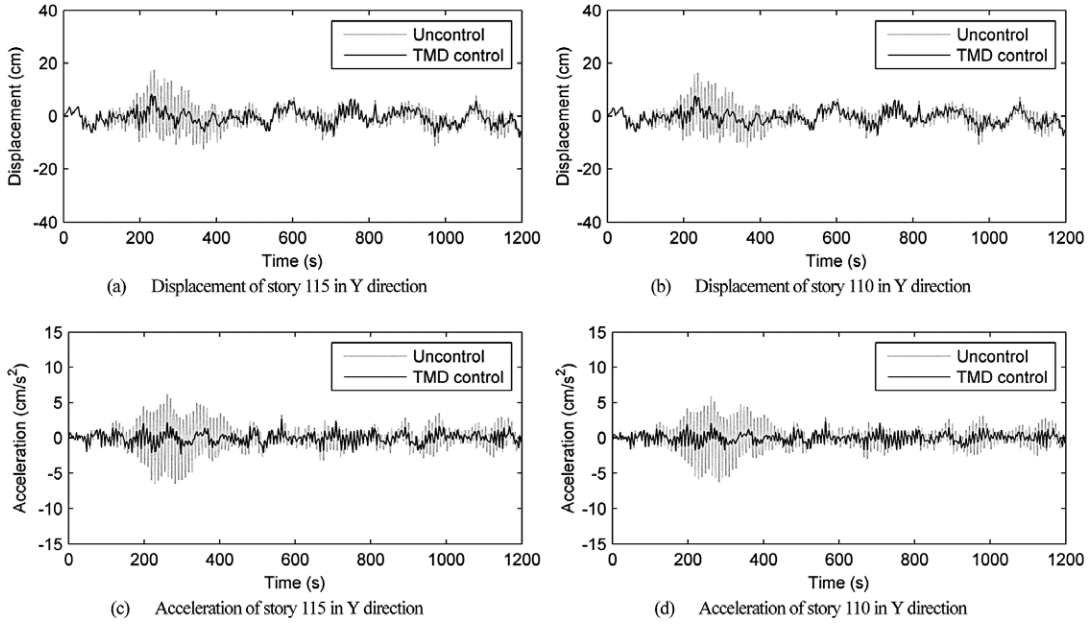

Figure 6. Time–history curves of structural response induced by one-year wind event in case 4.

5. CONCLUDING REMARKS

The wind-induced response of SHC and the wind vibration control performance are presented in the paper. The analysis results confirm the necessity and effectiveness of TMD systems for vibration mitigation of the SHC under wind excitation. The structural acceleration response induced by wind events of a 10-year return period will exceed the living comfort limit, which can be controlled to a large extent and be suppressed below the residential comfort criteria after the installation of the TMD

DOI: 10.1002/tal

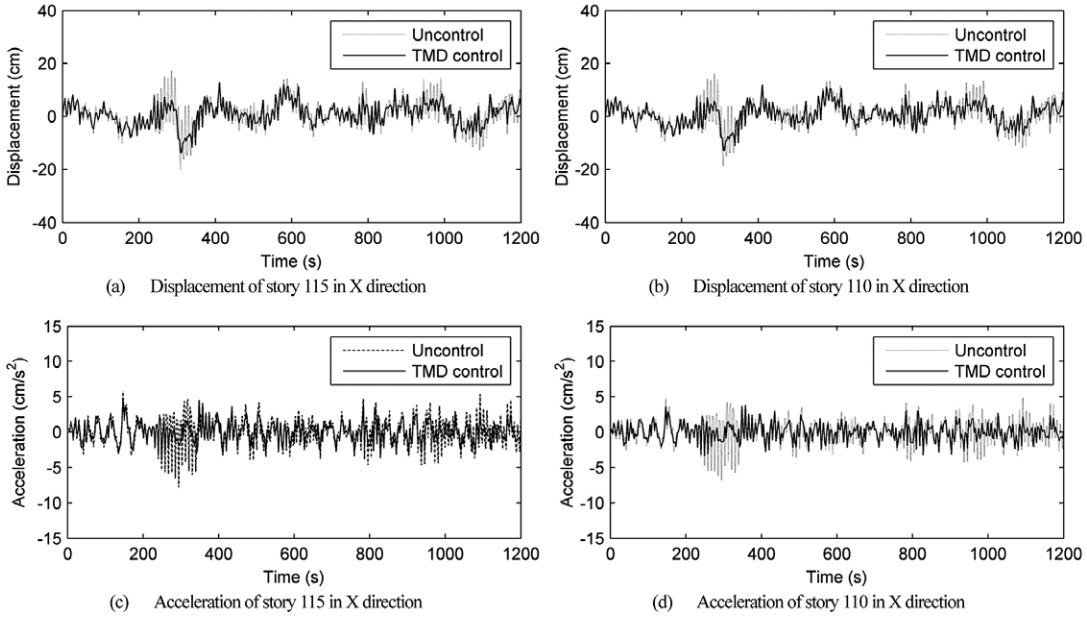

Figure 7. Time–history curves of structural response induced by 10-year wind event in case 1.

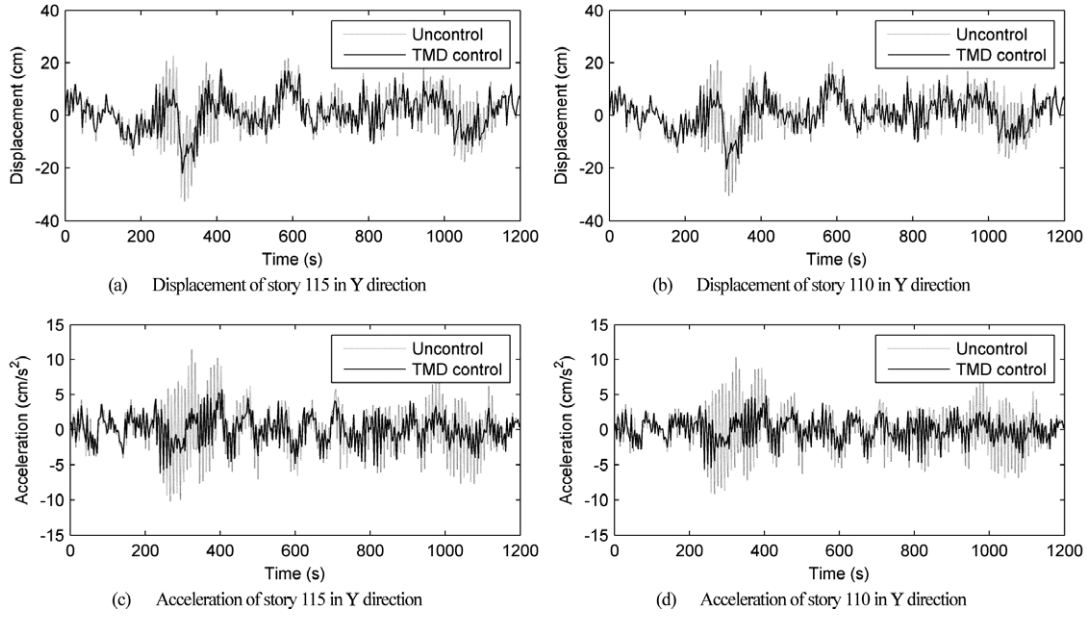

Figure 8. Time–history curves of structural response induced by 10-year wind event in case 4.

system. Besides, the TMD system also has a considerable influence on suppression of the structural wind-induced displacement response. The results demonstrated in this paper provide fundamentally important information for the vibration control design of the SHC in the future.

ACKNOWLEDGEMENTS

The research was partially supported by the Natural Science Foundation of China for Key Projects of Major Research Plan, Grant No. 90815029 and 51021140006. The authors also would like to

DOI: 10.1002/tal

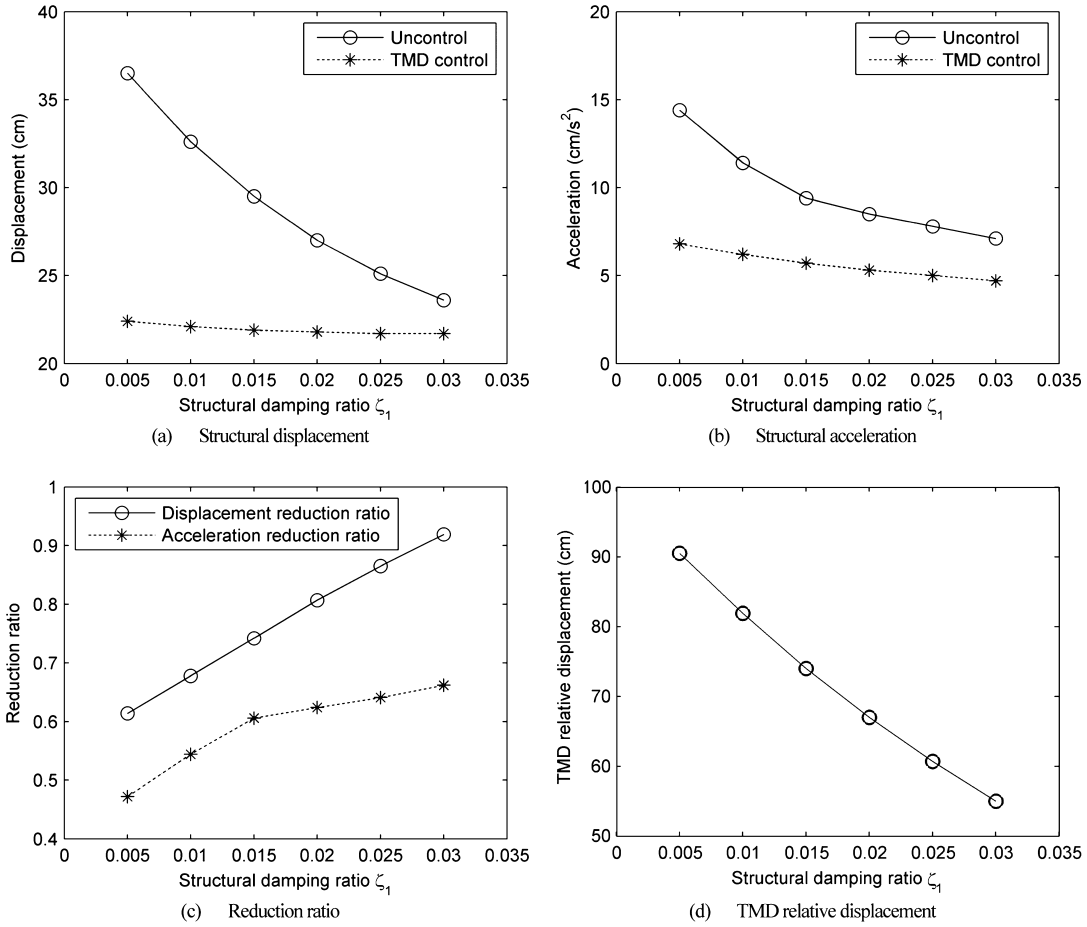

Figure 9. Relation between maximum response induced by 10-year wind event in case 4 and different structural damping ratios.

acknowledge the Architectural Design & Research Institute of Tongji University for providing the tower data.

REFERENCES

Clough RW, Penzien J. 1993. *Dynamics of Structures*. McGraw-Hill: New York.

Fujino Y, Soong TT, Spencer BF Jr. 1996. Structural control: basic concepts and applications. In *Proceedings of the 1996 ASCE Structures Congress*, Chicago, IL, April 15–18; **2**: 1277–1287.

Ghorbani-Tanha AK, Noorzad A, Rahimian M. 2009. Mitigation of wind-induced motion of Milad tower by tuned mass damper. *Structural Design of Tall and Special Buildings* **18**(4): 371–385.

Iannuzzi A, Spinelli P. 1987. Artificial wind generation and structural response. *Journal of Structural Engineering* **113**(12): 2382–2398.

Simiu E, Scanlan RH. 1996. *Wind Effects on Structures: Fundamentals and Applications to Design.* John Wiley: New York.

Smith R, Willford M. 2007. The damped outrigger concept for tall buildings. *Structural Design of Tall and Special Buildings* **16**: 501–517.

Smith R, Willford M. 2008. Damping in tall buildings—uncertainties and solutions. In *17th Congress of Iabse*, Chicago, IL, September 17–19; 1–8.

Soong TT, Dargush GF. 1997. *Passive Energy Dissipation Systems in Structural Engineering*. Wiley: Chichester.

DOI: 10.1002/tal